Current Applied Physics 14 (2014) 1703–1706

Contents lists available at ScienceDirect

Current Applied Physics

journal homepage: www.elsevier.com/locate/cap

Atomic layer deposited HfO_2 based metal insulator semiconductor GaN ultraviolet photodetectors

Manoj Kumar [a, *], Burak Tekcan [a, b], Ali Kemal Okyay [a, b, *]

[a] UNAM-National Nanotechnology Research Center and Institute of Materials Science and Nanotechnology, Bilkent University, 06800 Ankara, Turkey
[b] Department of Electrical and Electronics Engineering, Bilkent University, 06800 Ankara, Turkey

ARTICLE INFO

Article history:
Received 1 September 2014
Received in revised form
1 October 2014
Accepted 13 October 2014
Available online 13 October 2014

Keywords:
GaN
Atomic layer deposited HfO_2
UV photodetectors

ABSTRACT

A report on GaN based metal insulator semiconductor (MIS) ultraviolet (UV) photodetectors (PDs) with atomic layer deposited (ALD) 5-nm-thick HfO_2 insulating layer is presented. Very low dark current of 2.24×10^{-11} A and increased photo to dark current contrast ratio was achieved at 10 V. It was found that the dark current was drastically reduced by seven orders of magnitude at 10 V compared to samples without HfO_2 insulating layer. The observed decrease in dark current is attributed to the large barrier height which is due to introduction of HfO_2 insulating layer and the calculated barrier height was obtained as 0.95 eV. The peak responsivity of HfO_2 inserted device was 0.44 mA/W at bias voltage of 15 V.

1. Introduction

GaN has emerged as a potential candidate for fabrication of UV PDs due to its wide and direct band gap energy (3.4 eV) and high saturation velocity (3×10^7 cm/s). The advantage of excellent radiation hardness and high-temperature stability also make it a suitable material for UV detectors working in extreme conditions [1,2]. Moreover, GaN and its related ternary allows such as $Al_xGa_{1-x}N$ are very promising for the fabrication of high power and high frequency solid state electron devices due to the generation of two dimensional electron gas (2DEG) by the spontaneous and piezoelectric polarization charges in the AlGaN/GaN heterojunctions [3]. AlGaN/GaN based HEMTs is particularly attractive for next-generation RF/microwave power amplifiers due to its excellent performances in high temperature and high power operations at microwave frequencies [4]. Until now HEMTs, operating at high power densities and at frequencies up to several giga hertz have been reported [5]. Owing to small size, high performance and low cost characteristics of GaN based UV PDs, It is an appropriate candidate for various applications such as flame detection, missile warning and space monitoring [6–8]. Over the past few years, variety of GaN based PDs have been investigated such as p-i-n PDs, Schottky PDs and metal semiconductor metal (MSM) PDs, but most of them suffered from high leakage current [9–11]. Among them, MSM PD is most promising candidate for UV PDs applications due to its easy fabrication process, high speed and compatibility with electronic technology. The metals used for the fabrication of MSM PD device are not sufficiently stable and interdiffusion also occur at the metal GaN interface. In order to overcome large leakage current problem in MSM PDs and to avoid metal interdiffusion problem, insulator layer in between metal electrode and underlying semiconducting layer can be introduced. By utilizing appropriate insulating layer, larger barrier height at metal semiconductor interface can be achieved. Larger barrier height can lead to a lower leakage current and higher breakdown voltage, which may improve the device performance. In the recent past, many insulating materials such as SiO_2, Si_3N_4, ZrO_2 and Ga_2O_3 are commonly used for GaN based MIS UV PDs [12–15]. It is highly desirable for GaN PDs to have high-k oxide insulator which do not react with GaN layer. A high-k dielectric oxide with valence band offset higher than 1 eV has advantage to function as an appropriate insulator on GaN. Among such high-k oxide materials, HfO_2 is considered one of the most promising insulating material due to its high permittivity and band alignment properties. In the literature, however, there are few reports available focused on HfO_2 as an interfacial layer for GaN MIS UV PDs.

In this paper GaN based MIS UV PDs are demonstrated using a thin HfO_2 interfacial introduced between metal and underlying GaN layer. HfO_2 insulating layer is grown by ALD technique. The results show that the dark current is dramatically suppressed even

* Corresponding authors. UNAM-National Nanotechnology Research Center and Institute of Materials Science and Nanotechnology, Bilkent University, 06800 Ankara, Turkey.
E-mail addresses: aokyay@ee.bilkent.edu.tr, panwarm72@yahoo.com (A.K. Okyay).

http://dx.doi.org/10.1016/j.cap.2014.10.001
1567-1739/

at high applied voltage bias and photo-to-dark current ratio is found to be improved.

2. Experimental details

The GaN samples used in this work were commercially available and grown using metal organic chemical vapor deposition technique on sapphire. The epi-layer consisted of 1.2 μm Si doped GaN and 300 nm unintentionally doped GaN. The nominal Hall Effect measured carrier concentration was found to be 1.4×10^{18} and 1.1×10^{17} cm^{-3} respectively. GaN samples were cleaned using acetone and isopropyl alcohol and then unintentionally grown oxide layer was etched by buffered hydrofluoric acid. HfO_2 layer was deposited on top of the GaN in Ultratech/Cambridge Nanotech Savannah 100 ALD system with Tetrakis (Dimethylamido) Hafnium and H_2O as precursors. The base pressure was maintained at 1 Torr during deposition. The resulting thickness of interfacial HfO_2 layer was 5 nm.

Standard photolithography and lift-off processes were then obtained to define inter digitated contact electrodes. Fig. 1 illustrates the schematic structure of the fabricated GaN MIS PDs with HfO_2 insulating layers. Magnetron sputtered 10/100 nm thick Ni/Au inter digitated fingers (rectangular shaped of 5 × 110 μm with spacing of 10 μm) were fabricated on HfO_2/GaN samples. The deposition was carried out in a vacuum chamber evacuated at base of 5.6×10^{-6} Torr. High purity Ar was used as sputtering gas. During the Ni deposition power of 125 W, gas flow rate of 50 SCCM, deposition time of 1 min, and pressure of 20 mTorr were kept constant. Au was fabricated at constant power of 75 W, gas flow of 50 SCCM and pressure of 1 mTorr. The current–voltage (I–V) measurements were performed using semiconductor parameter analyzer (Keithley 4200) and Keithley 2400 Sourcemeter. The spectral response was obtained by using a lock-in amplifier (SRS820) with an optical chopper and a monochromator from 300 to 420 nm with a 150 W xenon arc lamp.

3. Results and discussion

The typical room temperature I–V characteristics of without and with HfO_2 interfacial layer of GaN UV PDs under dark and illuminated at 360 nm is illustrated in Fig. 2. The device fabricated with HfO_2 interfacial layer exhibited dark current as low as

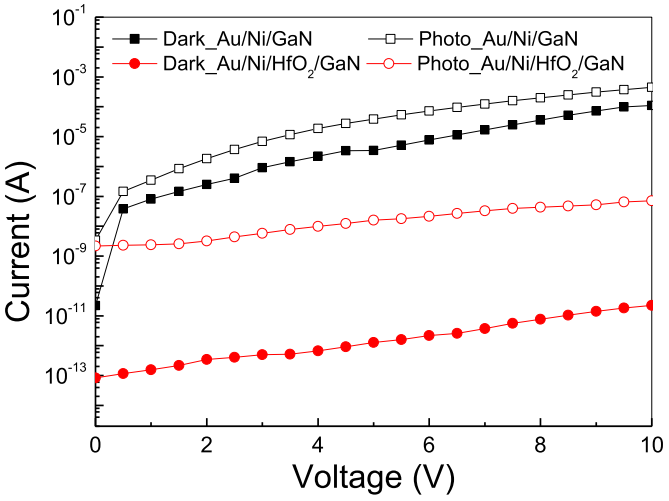

Fig. 2. Typical room temperature dark and photo I–V characteristics of without and with HfO_2 inserted in between metal and underlying GaN devices.

2.24×10^{-11} A at 10 V but the device prepared without HfO_2 revealed dark current of 1.1×10^{-4} A. It is believed that GaN surface is having high density of threading dislocations which accompanied by high leakage current. These dislocation densities contribute significantly more to the leakage current of the device. Li et al. [16] has studied the influenced of threading dislocations on the properties of GaN MSM UV PD and they observed that screw dislocations produce adverse effect on dark current. Screw dislocation is the path of carrier transportation. Same group further investigated to minimize the dislocations by depositing SiO_2 nanoparticles. It was found that SiO_2 nanoparticle was formed at the termination of screw and mixed dislocations, thereby effectively reduced leakage current [17]. The dramatically reduced dark current more than seven orders of magnitude was observed at a bias voltage of 10 V due to introduction of HfO_2 interfacial layer, indicating perfect insulating layer for GaN based devices. It was also found that this value is much superior to those observed from HfO_2, Al_2O_3 and GaO_x inserted MIS device [18–20]. It is believed that high-k dielectric HfO_2 insulating interfacial layer formed a high potential barrier between the metal and the GaN and thereby reducing the dark current. Furthermore, the HfO_2 interfacial layer play the role of

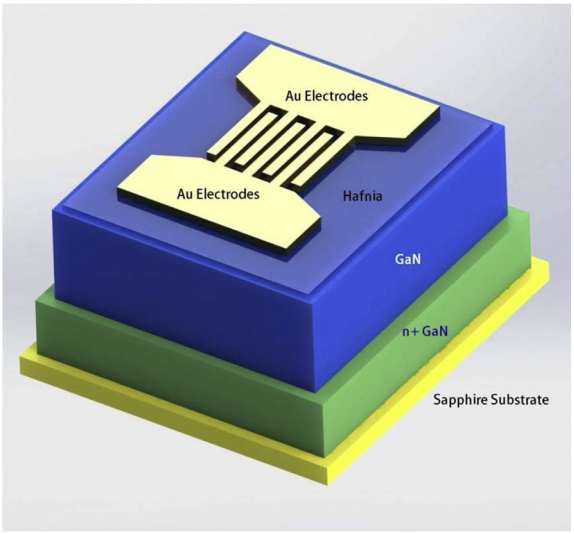

Fig. 1. Schematic illustration of fabricated GaN MIS PD with HfO_2 insulating layer.

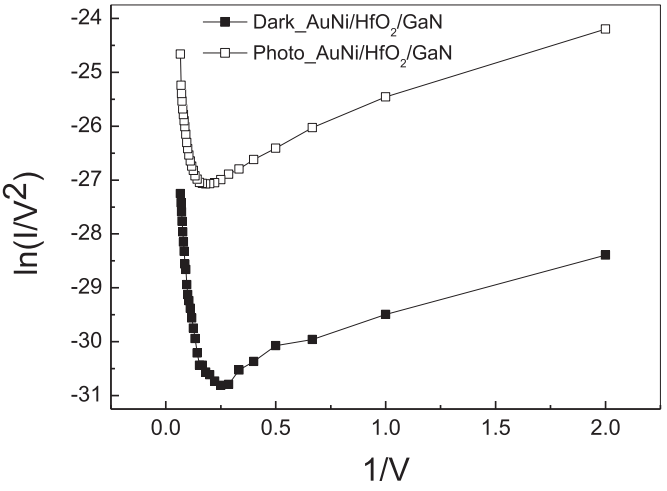

Fig. 3. F–N plot of forward dark and photo I–V characteristics of the HfO_2 introduced GaN MIS UV PD.

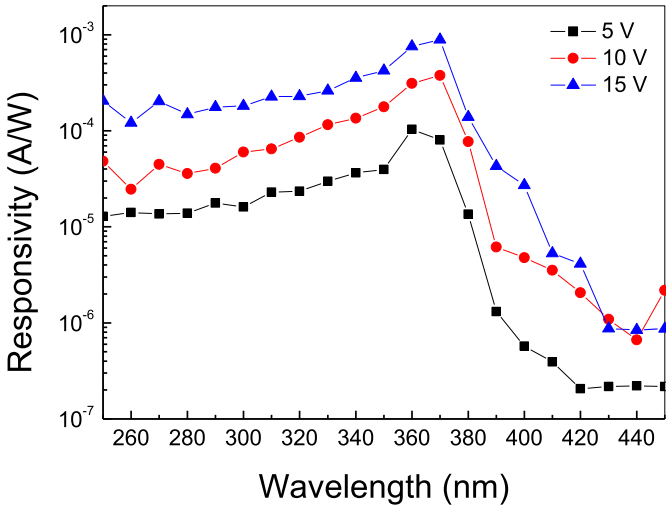

Fig. 4. Voltage dependent spectral responsivity of the HfO_2 introduced GaN MIS UV PD.

passivation layer to minimise the surface defects, thereby reducing the recombination events occurring at the metal/semiconductor interface during the light illumination. The barrier height (φ_b) and ideality factor (n) values were determined by using the thermionic emission theory. The barrier height of 0.95 eV and ideality factor of 1.31 were obtained from the forward I–V characteristics, respectively for the HfO_2 inserted GaN MIS UV PD. The obtained photo-to dark current contrast ratio was found to be about 10^3, which is relatively comparable of the reported results and furthermore, it is obtained to be more than two orders of magnitude higher than without HfO_2 device. Under illumination, the relative higher photo-to-dark-current ratio is observable in GaN MIS PD. The contrast ratio is around 2.62×10^3 at bias voltage of 10 V. At the same condition, the ratio obtained without HfO_2 insertion is only 3.36.

Fig. 3 shows the $\ln(I/V^2)$ versus $1/V$ plot of GaN MIS PD at forward bias. In both dark and illuminated conditions, Linear decrease of $\ln(I/V^2)$ vs $1/V$ was obtained at higher voltage region, confirming the F–N tunneling behavior. By expanding the F–N plot to the wider range of the voltage (higher voltage region to shorter voltage region), clear threshold voltage is appeared around 4–5 V from where transition of carrier transport from F–N to direct tunneling region was started. The F–N tunneling is obviously occurred at higher voltage might be the presence of higher interfacial surface states. Due to the existence of trap states which behave acceptor like nature, electrons would easily be gathered and formed surface charge region, which consequently enhances the probability of the electron hole recombination. This implies that at a higher applied voltage, the charge carriers may traverse through the sample because of narrowing of the potential barrier. F–N tunneling mechanism was found to be the main conduction mechanism in the MIS PDs at higher bias voltage in both conditions which is expressed by [21]

$$J_{FN} = V^2 \exp\left(\frac{B}{V} + A\right) \tag{1}$$

where A and B are constants given by $A = q^2/(8\pi h d^2 \varphi)$ and $B = 4\sqrt{2qm^* m_0 \varphi^{3/2}}/3\hbar$

In the above equation, φ stands for the barrier height in eV, m^* is the effective electron mass, d is the tunnel barrier width, m_o is the free electron rest mass, Q is the electron charge and $\hbar$ is the reduced Plank's constant.

Fig. 4 demonstrates bias dependent measured spectral responsivity of GaN MIS PDs. It is clearly seen from the Fig. that the spectral response evidently starts cut off from 370 nm. The cut-off wavelengths of GaN MIS PD are in good agreement with band gap energy of GaN. Owing to the insulating nature of HfO_2, photocurrent should decrease and thereby small responsivity was achieved from the fabricated MIS UV PD. The peak responsivity of 0.75 mA/W was achieved at bias voltage of 15 V. UV to visible rejection ratio was obtained to be more than three orders of magnitude as defined the responsivity measured at 370 nm divided by that measured at 440 nm. It is assumed that a higher trap density exists at the interface and/or deep in the HfO_2 which are more easily captured electrons injected from the metal. As a result, a trapped electron space charge region is formed. These trapped electrons act as hole traps and tend to capture photo generated holes from the GaN. Therefore, this trapping process increases the probability of the recombination of photo generated carriers at the interface, thereby low responsivity was obtained. The responsivity of 0.47 A/W was obtained at 5 V for without HfO_2 interfacial GaN UV PD. The obtained gain in the GaN UV PD without HfO_2 insulating layer may be due to the higher mobility and their transit time shorter than the carrier life time of the majority carriers. Meantime, the minority carriers are slower and their transit time is longer than the carrier life time. Under this circumstance, electrons are moved out of the detector quickly but the holes demand charge neutrality and more electrons are supplied from the other electrode. However, electrons go many times through the detector during the carrier life time and thereby this action is producing gain. Considerable bias-dependent spectral response was observed from the GaN MIS PD, which can be

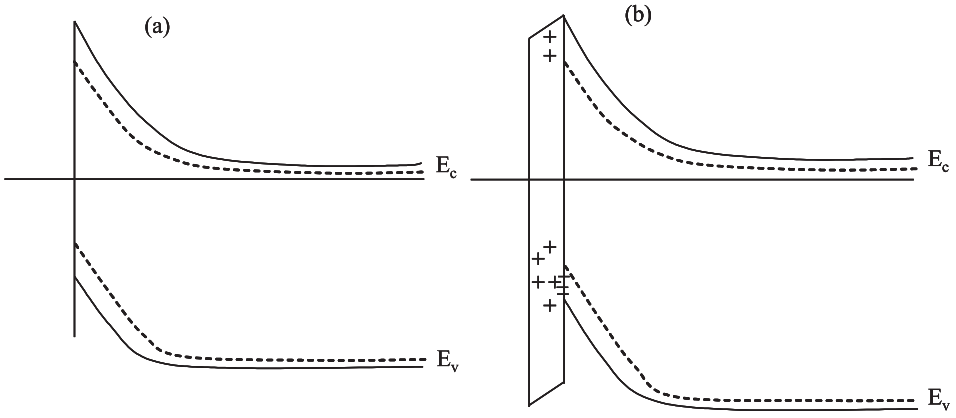

Fig. 5. Qualitative band diagram of the HfO_2 introduced GaN MIS UV PD.

attributed to the photoresponse caused from the defects at the interface of GaN MIS PD as is shown in Fig. 5. This phenomenon occurs, especially when the bias voltage increased because of the barrier thickness decreases, thereby enhancing trap assisted tunneling of photo generated carriers. The discrepancy between forward and reverse bias I–V characteristics of GaN MIS PD was also noticed, which may be possibly attributed to the trapping of the photocarriers by the deep traps in HfO_2 and/or GaN layer during their F–N tunneling. A thin and higher barrier was established after the introduction of HfO_2 between metal and underlying GaN. The GaN MIS PD required stronger electric field to enable the photocarriers to tunnel the barrier. The sufficient photo generated carriers could not tunnel through because this bias is not sufficient to reduce the barrier effectively. However, some of photocarriers are contributed to the current. Clearly, small bias dependent spectral response was obtained.

The detectivity of the device is calculated by assuming the source of noise is thermally limited and the background radiation is very low and is expressed as [22]

$$D = R\left(\frac{R_0 A}{4kT}\right)^{\frac{1}{2}} \tag{2}$$

where R is the zero bias reponsivity, R_0 is the differential resistance at zero bias and A is the detector area. The differential resistance was calculated by taking the derivative(dV/dI) of the resulting curves of the GaN MIS PD. The differential resistance of the PD was calculated by taking the (dV/dI) derivative and obtained values of 2.17×10^{13} Ω, resulting in the R_0A product of 5.98×10^8 Ω-cm^2. The detectivity performance of the GaN MIS PD of 1.89×10^{12} cm Hz$^{1/2}$ W^{-1} was achieved. The obtained results are better than those of previously reported GaN based MSM PDS [23,24].

4. Conclusion

ALD grown HfO_2 interfacial layer inserted GaN MIS UV PD was demonstrated. The device achieved a low dark current and larger dark-to-photo current contrast ratio. The dark current was found to reduce by seven orders of magnitude. Measured responsivity value of 0.44 mA/W was achieved and a device detectivity value of 1.89×10^{12} cm Hz$^{1/2}$ W^{-1} was obtained. These results indicate great potential for the use of ALD grown HfO_2 as an insulator layer for MSM UV PD devices.

Acknowledgment

This work was supported by the Scientific and Technological Research Council of Turkey (TUBITAK), grant numbers 109E044, 112M004, 112E052, and 113M815. A. K. O. acknowledges support from European Union FP7 Marie Curie International Reintegration Grant (PIOS, Grant # PIRG04-GA-2008-239444). A.K.O. acknowledges support from the Turkish Academy of Sciences Distinguished Young Scientist Award (TUBA GEBIP).

References

[1] T. Sawada, Y. Ito, K. Imai, K. Suzuki, H. Tomozawa, S. Sakai, Appl. Surf. Sci. 159 (2000) 449.
[2] D. Li, X. Sun, H. Song, Z. Li, H. Jiang, Y. Chen, G. Miao, B. Shen, Appl. Phys. Lett. 99 (2011) 261102.
[3] T. Palacios, A. Chakraborty, S. Rajan, C. Poblenz, S. Keller, S.P. DenBaars, J.S. Speck, U.K. Mishra, Electron Dev. Lett. 26 (2005) 781.
[4] X. Wang, W. Hu, X. Chen, W. Lu, Trans. Electron Dev. 59 (2012) 1393.
[5] M. Yanagihara, Y. Uemoto, T. Ueda, T. Tanaka, D. Ueda, Phys. Status Solidi A 206 (2009) 1221.
[6] G. Hellings, J. John, A. Lorenz, P. Malinowski, R. Mertens, IEEE Trans. Electron Devices 56 (2009) 2833.
[7] M. Asif Khan, M. shatalov, H.P. Maruska, H.M. Wang, E. Kuokstis, Jpn. J. Appl. Phys. Part 1 44 (2005) 7191.
[8] E. Kim, B. Lee, A. Nahhas, H.K. Kim, Appl. Phys. Lett. 77 (2000) 1747.
[9] X.D. Wang, W.D. Hu, X.S. Chen, J.T. Xu, X.Y. Li, W. Lu, Opt. Quantum Electron 42 (2011) 755.
[10] M. Kumar, C.Y. Lee, H. Sekiguchi, H. Okada, A. Wakahara, Semicond. Sci. Technol. 28 (2013) 094005.
[11] Y.K. Su, S.J. Chang, C.H. Chen, J.F. Chen, G.C. Chi, J.K. Sheu, W.C. Lai, J.M. Tsai, IEEE Sens. J. 2 (2002) 366.
[12] C.H. Chen, Y.H. Tsai, S.Y. Tsai, C.F. Cheng, Jpn. J. Appl. Phys. 50 (2011) 04DG19.
[13] Z.G. Shao, D.J. Chen, B. Liu, H. Lu, Z.L. Xie, R. Zhang, Y.D. Zheng, J. Vac. Sci. Technol. B 29 (2011) 051201-1.
[14] Y.Z. Chiou, J. Electrochem. Soc. 152 (2005) G639.
[15] Z.D. Huang, W.Y. Weng, S.J. Chang, Y.F. Hua, C.J. Chiu, T.Y. Tsai, Photonic Technol. Lett. 25 (2013) 1809.
[16] D. Li, X. Sun, H. Song, Z. Li, Y. Chen, G. Miao, H. Jiang, Appl. Phys. Lett. 98 (2011) 011108.
[17] X. Sun, D. Li, H. Jiang, Z. Li, H. Song, Y. Chen, G. Miao, Appl. Phys. Lett. 98 (2011) 121117.
[18] C.H. Chen, Jpn. J. Appl. Phys. 52 (2013) 08JF08.
[19] C.J. Lee, Y.J. Kwon, C.H. Won, J.H. Lee, S.H. Hahm, Appl. Phys. Lett. 103 (2013) 111110.
[20] M.L. Lee, T.S. Mue, F.W. Huang, J.H. Yang, J.K. Sheu, Opt. Exp. 11 (2011) 12658.
[21] M. Liao, X. Wang, T. Teraji, S. Koizumi, Y. Koide, Phys. Rev. B 81 (2010) 033304.
[22] S.J. Chang, T.K. Ko, J.K. Sheu, S.C. Shei, W.C. Lai, Y.Z. Chiou, Y.C. Lin, C.S. Chang, W.S. Chen, C.F. Shen, Sensors Actuators A 135 (2007) 502.
[23] Y.K. Su, P.C. Chang, C.H. Chen, S.J. Chang, C.L. Yu, C.T. Lee, H.Y. Lee, J. Gong, P.C. Chen, C.H. Wang, Solid State Electron 49 (2005) 459.
[24] R.W. Chuang, S.P. Chang, S.J. Chang, Y.Z. Chiou, C.Y. Lu, T.K. Lin, Y.C. Lin, C.F. Kuo, H.M. Chang, J. Appl. Phys. 102 (2007) 073110.